View metadata, citation and similar papers at core.ac.uk
brought to you by CORE

GEOFIZIKA VOL. 15 1998

Original scientific paper
UDC 551.511

The energy cycle in a cyclone over the Bay of Genoa

Ivana Herceg

Andrija Mohorovičić Geophysical Institute, Faculty of Science, University of Zagreb

Received 12 February 1998, in final form 9 October 1998

Zonal available potential energy, eddy available potential energy, eddy kinetic energy and conversion of zonal to eddy potential energy have been evaluated for the period from 5 to 15 February 1986 using data from Wetterbericht charts. These terms were calculated for a limited domain ranging from 40 °N to 50 °N latitude and from 5 °E to 20 °E longitude. A cyclone developed over the Bay of Genoa during the considered period. The system formed simultaneously at all levels in the troposphere as was noticeable on the synoptic charts. The cyclone life cycle could be described by time variations of the eddy available potential energy, since it increased during the intensifying and decreased during the weakening stage of the system.

A stability diagram has been used to examine connection of the cyclone amplification and calculated energy terms with conditions in the atmosphere presented by critical meridional temperature gradient. The results obtained by the stability diagram correspond to energy estimations. In those days for which the stability diagram indicated amplification of the cyclone, the eddy energy terms increased and so the cyclone growth was evident on the synoptic charts.

Keywords: available potential energy, kinetic energy, energy transformation, eddy, cyclone, stability diagram.

1. Introduction

The idea of available potential energy was given by Margules (1903). It represents that part of the potential energy which can be transformed into kinetic energy. Lorenz (1955) explained its application to the general circulation of atmosphere. The basic state of the atmosphere is a very sensitive balance between the symmetric zonal and wavy regimes. A large scale flow can be examined as a zonal flow with disturbances superimposed on it. Therefore available potential energy (A) can be resolved into a zonal (A_Z) and an eddy (A_E) component. Kinetic energy also can be partitioned into zonal (K_Z) and eddy (K_E) kinetic energy. Differential heating of the hemisphere acts as a source of zonal available potential energy, *i.e.* A_Z is generated by low-latitude

heating and high-latitude cooling. A_E is generated, or dissipated, by local heating or cooling. A_Z, A_E, K_Z and K_E interact by their redistributions. Thus A_E acts as a source of K_E, while K_Z maintenance is due to a direct transformation of A_Z and also due to energy redistribution from eddies to the zonal flow. Both components of kinetic energy are dissipated by friction. Analytic expressions for energy generation, dissipation and energy conversions were given by Lorenz (1955). Although his theory was developed in the first place for studying the global atmosphere energy cycle, some authors applied it to relatively small regions, particularly with respect to monsoon development (Desai, 1986; Rajamani and Kulkarni, 1986; Singh and Singh, 1992). Šinik (1986) showed that the process of energy transformation $C(A_Z,A_E)$ could be estimated by means of a cospectral function and if it was determined for a limited region, it might help in forecasting of a given eddy scale development. However, the theory of the global energy cycle has been developed by the assumption that the atmosphere is a closed system with a constant sum of potential and kinetic energy. Since the atmosphere over a limited region is not a closed system, energy conservation may not be satisfied. Furthermore, determination of energy terms requires calculating of area and zonal means and deviations from them for the whole atmosphere. That can not be managed in the case of a small domain where calculated mean values refer to the limited region under the study. Still, one can expect that some applications of the mentioned theory on the smaller regions would give logical results if examined disturbances act as closed systems where the properties of the energy conservation are kept. In such conditions it can be expected that the disturbance growing (weakening) would be followed by an increase (decrease) of the corresponding eddy energy terms. That was exactly the case with the cyclone described in this paper.

Cyclones formed over the Bay of Genoa have a strong influence on the weather in south-east European region. Srnec (1996) found that such cyclone development during the period from 9 to 15 February 1986 markedly effected the planetary boundary layer over north-western Croatia.

This paper presents some results of energetic calculations of A_Z, A_E, and K_E during the life cycle of the cyclone formed over the Bay of Genoa. The complete study of some disturbance requires calculating all of energy terms, *i.e.* energy generation, kinetic and available potential energies of the zonal flow and eddies and their conversions, but the available data allowed us to determine only some of those quantities in this work. The purpose of the study is to find out whether the life cycle of a cyclone can be described in terms of the energy conversions for a relatively small region and makes the first attempt to estimate the energetics of a cyclone development over the considered region. A stability diagram (Labović, 1965) has been used to examine a dependence of the cyclone amplification upon the given static stability and meridional temperature gradient (the diagram makes it possible to determine the

critical value of meridional temperature gradient, $(\partial T/\partial y)_C$, over which a given perturbation could amplify). Mann and Šinik (1990) used a similar comparison of the theoretical $(\partial T/\partial y)_C$ with the observed $\partial T/\partial y$ in a study of hydrodynamic instability.

2. Synoptic situation and data

All of the data required for the estimation of A_Z, A_E, K_E, $C(A_Z, A_E)$ and input data for the stability diagram have been calculated for the time period from 5 to 15 February 1986. The cyclone has developed in the Bay of Genoa during that period. Data analysis showed that the cyclone evolution was sustained throughout the whole atmosphere. In the stage of its intensive development, the vertical axis of cyclone was inclined toward the west indicating a possibility of its further evolution. The minimum surface pressure (995 hPa) in the considered region was measured on 9 February (Fig. 1) and from that day onwards, the cyclone weakening was noticeable on the synoptic charts.

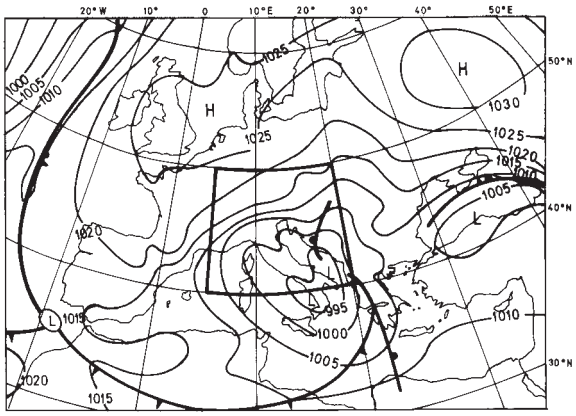

Figure 1. Synoptic situation on 9 Feb. 1986 at 1200 UTC. The area under the study is rounded by bold line.

To get the input data, Wetterbericht charts at 00 UTC were used (surface, 850 hPa, 700 hPa, 500 hPa, 300 hPa, 200 hPa and 100 hPa levels). Grid point values of the geopotential height and temperature at every 5-degree lat./long. grid were picked out over the region from 5 °E to 20 °E and from 40 °N to 50 °N. Figure 1 shows the synoptic situation on 9 Feb. 1986 at 1200 UTC, with bold lines indicating the grid contours. An additional experiment performed by the use of a grid with higher resolution did not improve the results significantly. Since the aim of the study was an examination of cyclone

influence upon the energetics of a limited region with a special reference to the area of Croatia, the region was defined as it can be seen on Fig. 1.

Geostrophic assumption was used to calculate meridional wind components. Derivatives were obtained by using the centred finite difference method. Integrations were performed in the vertical from 1000 hPa to 100 hPa, in 100 hPa steps using the trapezoidal rule.

3. Equations

The A_E, K_E, $C(A_Z, A_E)$ and input data for stability diagram have been calculated using the following equations:

– meridional component of geostrophic wind

$$v = \frac{g}{fa\cos\varphi}\frac{\partial Z}{\partial \lambda} \tag{1}$$

– zonal available potential energy

$$A_Z = \frac{1}{2}C_p \int_M \gamma [T]''^2 \, \mathrm{d}M \tag{2}$$

– eddy available potential energy

$$A_E = \frac{1}{2}C_p \int_M \gamma [T^{*2}] \mathrm{d}M \tag{3}$$

– eddy kinetic energy

$$K_E = \frac{1}{2}\int_M [v^{*2}] \mathrm{d}M \tag{4}$$

– transformation from zonal to eddy available potential energy

$$C(A_Z, A_E) = -C_P \int_M [v^* T^*] \frac{\partial [T]}{a\,\partial \varphi} \mathrm{d}M \tag{5}$$

– stability factor

$$\gamma = -\frac{\Theta R}{C_p T p}\left(\frac{\partial \overline{\Theta}}{\partial p}\right)^{-1} \tag{6}$$

– static stability parameter

$$s = \delta - \Gamma \tag{7}$$

where:
Z – geopotential height
dM – increment of mass,
δ – adiabatic lapse rate,
Γ – vertical rate of change of potential temperature,
and a, φ, λ, g, f, T, Θ, C_P, R, p, have their conventional meteorological meanings.

If X is an arbitrary variable, then the following notation is used:
$[X]$ – average in the zonal direction over the domain,
$\overline{X}$ – area mean over the considered area,
$X^* = X - [X]$ – deviation from the aforesaid zonal mean,
$[X]' = [X] - \overline{X}$ – deviation of the zonal mean from the area mean.

4. Results and discussion

4.1. Zonal and eddy available potential energy

The A_E generation was not calculated here because of lack of required data. But, A_E also can change due to a transformation $C(A_Z,A_E)$ from A_Z. The physical mechanism of this transformation is a meridional transport of sensible heat ($[v^*T^*]$) due to the existence of a temperature gradient over the region (see Eq. 5). Thus, an increase of A_E accompanied with positive $C(A_Z,A_E)$ has to be followed by decrease of A_Z because the disturbance receives energy from zonal flow and intensifies. Still, a comparison of variations of A_Z, A_E and $C(A_Z,A_E)$ on Figs. 2 and 3 shows that an increase of A_E is not always related to a simultaneous decrease of A_Z, as it might be expected. This is presumably due to the fact that the estimation of A_Z by the use of (2) was performed by data picked out from the limited region, not from the whole atmosphere.

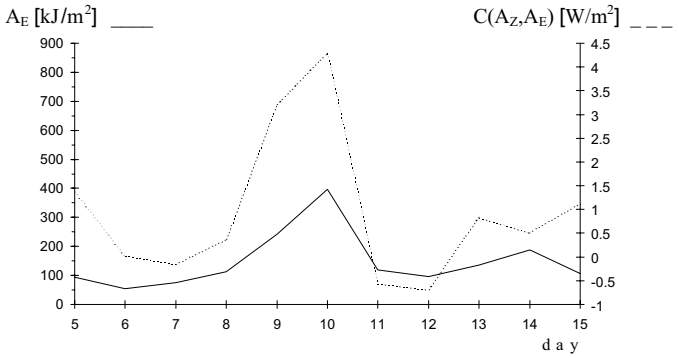

Figure 2. Eddy available potential energy (heavy line) and transformation from zonal to eddy available potential energy (dashed line) during the considered time period.

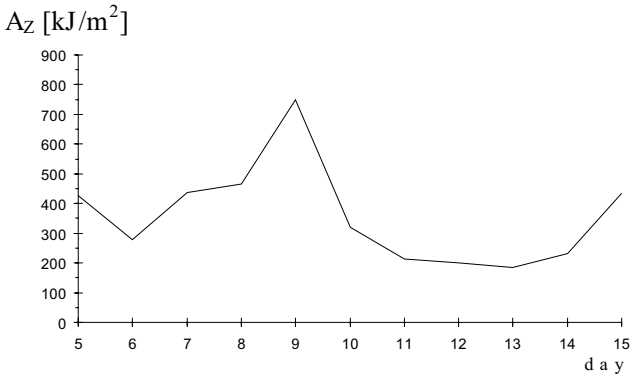

Figure 3. Zonal available potential energy during the considered time period.

4.2. Eddy kinetic energy

After the disturbance development due to its generation by temperature and diabatic heating differences and an energy transformation $C(A_Z,A_E)$, a part of the eddy available potential energy, A_E, is converted into the eddy kinetic energy, K_E, by means of vertical motions. K_E depends on deviations of both the meridional and the zonal components from the mean zonal flow over domain. But, having no knowledge on the mean zonal velocity because the domain is too small to calculate zonal winds, (*i.e.* we assumed that meridional components deviations have the main contribution to the K_E), so the eddy kinetic energy has been estimated only by introducing meridional wind components into the (4). Therefore, obtained results underestimate the real K_E, but they still allow making some conclusions about the K_E changes during the considered period. Fig. 4 illustrates that the eddy kinetic energy of

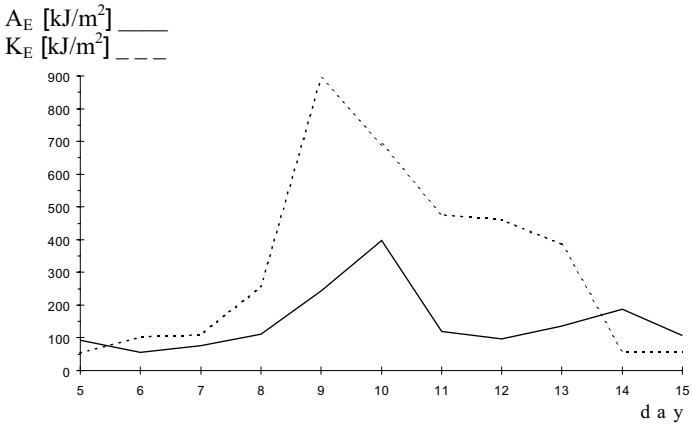

Figure 4. Eddy available potential energy (heavy line) and eddy kinetic energy (dashed line) during the considered time period.

the cyclone was mostly larger than the eddy available potential energy, what proves an efficient energy conversion $C(A_E,K_E)$ all the time.

K_E increased from the beginning of the considered period until 9 Feb. 1986 when it reached the maximum. Since K_E increases due to conversion of A_E into K_E, it can be expected that the increase of K_E would be coupled by a simultaneous decrease of A_E. Still, it is noticeable on Fig. 4 that the eddy available potential energy also increased during that period. Such behaviour of A_E indicates that its generation by local temperature and diabatic heating differences and its increase due to $C(A_Z,A_E)$ has been powerful enough to compensate the loss caused by its conversion into K_E. Eddy kinetic energy reached the maximum on 9 Feb. when the cyclone was matured, what can be seen on all synoptic charts for that day. Numerical values of the eddy potential (A_E) to eddy kinetic (K_E) energy conversion, could not be directly calculated in this study, since $C(A_E,K_E)$ is given by covariances of the unknown vertical velocity, ω, and specific volume, α, within latitude circles. Therefore, only the described comparison of A_E and K_E time changes during the considered period enabled an estimation of $C(A_E,K_E)$.

The most intensive accretion of K_E took place on 8 and 9 Feb. 1986 when snowfall was registered even at the island Rab, Croatia, what is a rarity there. Obviously, the conversion of A_E to K_E, accompanied by the rising of air and condensation was intense enough to cause rain and snow over the considered region. Calculated eddy terms increased during the cyclone development, and decreased during its weakening.

4.3. Stability diagram

The use of the so called 'stability diagram' allows to examine possibilities of the general circulation to change from symmetric to wave regimes. Suppose that general circulation is in the symmetric regime. Due to differential heating of the Earth, meridional temperature differences enhance up to their critical values above which the zonal flow becomes wavy. These waves make the meridional air mixing possible, with a consequent decrease of the temperature difference which was the primary reason for its creation. The stability diagram (Fig. 5) enables an estimation of the critical temperature gradient, $(\partial T/\partial y)_C$, for which, under given static stability conditions, zonal flow becomes unstable and the general circulation wave regime can take place.

The curves on the stability diagram denote 'critical state' for the given static stability. Outer sides of the curves belong to a region where the zonal flow is stable. Inside of the critical curves the flow is unstable. To determine if a disturbance superimposed on the zonal flow can amplify or not, its wavelength and static stability have to be given. For example, if measured meridional temperature gradient is –0.3 °C/°φ and static stability is –2.5 °C/100 hPa, than one can find on the Fig. 5 that disturbances with wavelengths

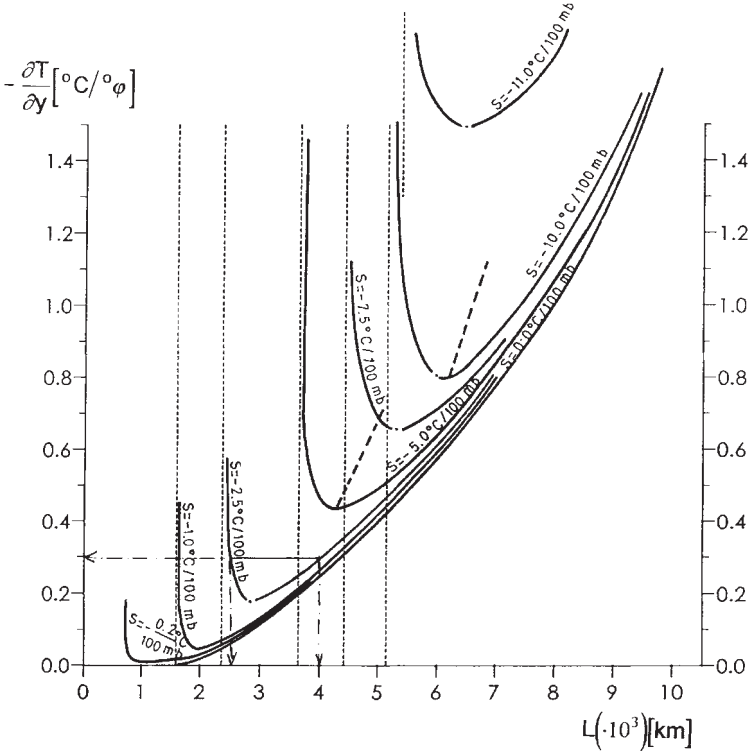

Figure 5. Stability diagram (from Labović, 1965).

within the interval from 2500 km to 4000 km can amplify. Disturbances outside of the aforementioned wavelength interval can not amplify because the conditions in the atmosphere attenuate their development. The diagram used in this work (Labović, 1965) can be applied for input data which refer to latitudes around 45 °N and 500 hPa pressure level. It has been used here to evaluate the dependence of a disturbance development on the static stability and meridional temperature gradient at 500 hPa level.

Table 1 contains static stability (s), meridional temperature gradient ($\partial T/\partial y$), wavelength (L) range of disturbances which can intensify (obtained from the stability diagram) and wavelengths (L_0) of the observed disturbance in the considered time period. Disturbance wavelengths were estimated from the synoptic charts (Wetterbericht, 1986).

During the cyclone formation period, estimated wavelengths were within the range of wavelengths that could amplify so the cyclone received energy from the zonal flow and grew. From 10 to 13 Feb. there were no wavelengths of any disturbances that could amplify and the cyclone dissipated. During

Table 1. *Static stability (s), meridional temperature gradient ($\partial T/\partial y$), wavelengths of disturbances which could amplify (L) and wavelengths of observed disturbance (L_0) during the period 5–15 February 1986.*

day	5	6	7	8	9	10	11	12	13	14	15
s [C/100 hPa]	–1.5	–1.6	–1.9	–2.9	–3.4	–4.7	–3.5	–2.9	–3.4	–3.0	–2.5
$\partial T/\partial y$ [°C/1 °φ]	–0.9	–0.3	–0.3	–0.4	–0.6	–0.4	–0.2	–0.2	–0.1	–0.5	–0.9
L [10^3 km]	2.0 7.0	2.0 4.0	2.3 4.5	2.7 4.5	3.0 6.0	–	–	–	–	3.0 5.0	2.5 6.0
L_0 [10^3 km]	3.2	2.2	2.7	3.9	4.0	3.3	2.8	2.3	1.2	1.1	7.8

that period, A_E decreased due to the conversion into K_E, so then less and less of energy was available for such conversion and the cyclone began to weaken. Since simultaneously the zonal flow began to receive the energy back from eddies and to strengthen, thus the energy cycle (formation, maturation and dissipation) of the cyclone was completed.

5. Conclusions

The presented case of the cyclone formation, maturation and dissipation is an example of the application of general circulation energetics to a relatively small region. Since the cyclone acted approximately as a closed system, its interactions with the surrounding atmosphere appeared to be negligible and the use of Eqs. 1 to 7 has given the logical and explainable results.

Calculations and comparisons of A_E and K_E showed that during cyclone development the local generation of the eddy available potential energy plus the $C(A_Z,A_E)$ was large enough to compensate the loss of A_E due to its conversion to K_E.

Both A_E and K_E were increasing during the development stage of the cyclone, and they began to decrease when the cyclone weakening was noticeable on the synoptic charts. The eddy kinetic energy was greater than eddy available potential energy implying an intense rising of warm air and sinking of cold air.

$C(A_Z,A_E)$ described logically a development of the cyclone, and it increased during the cyclone formation stage. As A_Z was not decreasing at the same time, it can be concluded that the estimation of zonal available potential energy for our small region was not reliable.

Results obtained by the use of the stability diagram are consistent with those of energy calculations during the considered synoptic situation. On those days for which the stability diagram indicated a possible cyclone amplification, the eddy energy terms increased and the cyclone development was strong.

Generally, the energy terms and conversions calculations in the presence of a depression may help in investigations of cyclone behaviours over different limited regions.

Acknowledgement. – The author is thankful to Prof. Nadežda Šinik for discussions and advising.

References

Desai, D. S. (1986): Study of energetics in strong and break monsoon, Mausam, **37**, 3, 365–367.

Gupta, S. C. and Mandal, G. S. (1987): Behaviour of kinetic energy generation function during a western disturbance in May 1982, Mausam, **38**, 97–102.

Holopainen, E.O. (1970): An observational study of the energy balance of stationary disturbances in the atmosphere, Quarterly Journal of Royal Meteorological Society, **96**, 626–644.

Labović, N. (1965): Dynamic instability in atmospheric macroscale motions, Zbornik meteoroloških i hidroloških radova, **2**, 8–17, (in Croatian).

Lorenz, E. N. (1955): Available potential energy and the maintenance of the general circulation, Tellus, **7**, 157–167.

Mann, M., and Šinik, N. (1990): Some properties of hydrodynamic instability in a quasi-geostrophic atmosphere, Geofizika, **7**, 55–70.

Oort, A. H. (1964): On estimates of the atmospheric energy cycle, Monthly Weather Review 92, 11, 483–493.

Rajamani, S. and Kulkarni, J. R. (1986): On some energy aspects of the monsoon depression during its life cycle, Mausam, **37**, 9–16.

Singh, U. S. and Singh, R. K. (1992): Study of available potential energy of depression pattern in the region of Bay of Bengal, Időjárás, **96**, 2, 93–105.

Srnec, L. (1996): Interaction of quasi-geostrophic atmosphere and planetary boundary layer, Bachelor's thesis (in Croatian).

Šinik, N., (1986): One-dimensional spectral analysis of the available potential energy growth over a limited region, Geofizika, **3**, 23–33.

Wiin-Nielsen, A., Brown J. A. and Drake, M. (1963): On atmospheric energy conversions between the zonal flow and the eddies, Tellus, **15**, 3, 261–279.

Europischer Wetterbericht, Amstblatt des Deutschen Wetterdienstes (1986).

SAŽETAK

Energetski ciklus genovske ciklone

Ivana Herceg

Zonalna raspoloživa potencijalna energija, raspoloživa potencijalna energija makroporemećaja, kinetička energija makroporemećaja i transformacija zonalne raspoložive potencijalne energije u raspoloživu potencijalnu energiju makroporemećaja proračunati su za period od 5. do 15. veljače 1986. na temelju podataka dobivenih pomoću Wetterbericht sinoptičkih karata. U tom je periodu došlo do formiranja Genovske ciklone čiji je razvoj istovremeno uočljiv kako na prizemnim, tako i na visinskim sinoptičkim kartama. Raspoloživa potencijalna energija makroporemećaja povećavala

se tijekom perioda jačanja ciklone, a smanjivala se tijekom njenog slabljenja, pa se razvoj ciklone može pratiti promjenama te veličine.

Korišten je i dijagram stabilnosti za procjenu povezanosti razvoja ciklone i njene energetike s uvjetima u atmosferi prikazanim pomoću kritičnog meridionalnog gradijenta temperature. Analiza rezultata pokazala je da razmatranje razvoja ciklone pomoću dijagrama stabilnosti odgovara energetskim procjenama. Naime, onih dana kad je dijagram stabilnosti ukazivao na povoljne uvjete za jačanje ciklone, također se povećavala i energija makroporemećaja.

Author's address: Ivana Herceg, Andrija Mohorovičić Geophysical Institute, Faculty of Science, University of Zagreb, Horvatovac bb, 10000 Zagreb, Croatia, (E-mail: iherceg@rudjer.irb.hr)